Interpretation of the Binding Energy and Auger Parameter Shifts Found by XPS for TiO_2 Supported on Different Surfaces

J. A. Mejías, V. M. Jiménez, G. Lassaletta, A. Fernández, J. P. Espinós, and A. R. González-Elipe*

Instituto de Ciencia de Materiales de Sevilla (CSIC-Universidad de Sevilla) and Dpto. Química Inorgánica, P.O. Box 1115, 41080 Sevilla, Spain

Received: April 2, 1996; In Final Form: July 11, 1996[⊗]

In this paper the deposition of very thin films of TiO_2 on different substrates (SiO_2, MgO, Ag) is studied by XPS. Shifts in the Ti 2p BE and the Auger parameter of Ti ($\alpha' =$ Ti 2p BE + Ti $L_3M_{23}V$ Auger KE) are observed on the three substrates. The magnitude and the sign of the shifts with respect to those of bulk TiO_2 depend on coverage and on the type of substrate. In a parallel way, the magnitude of the energy gap of thin films of TiO_2 changes depending on the substrate. This has been shown by UV−vis absorption spectroscopy for TiO_2 deposited on SiO_2 for a TiO_2−Ag "cermet" (ceramic−metal thin film) and by photoemission with synchrotron radiation for TiO_2 deposited on SiO_2. It is proposed that the shift in the Auger parameter and the energy gap of TiO_2 in these systems are two related parameters. Molecular orbital calculations (extended Hückel and INDO/1) with clusters simulating the TiO_2−substrate interface explain qualitatively the variations in the Auger parameter and in the energy gap. The contribution of the polarization of the medium to the changes in the Auger parameter is approximated with an electrostatic model that accounts for the influence of the support in the observed shifts.

Introduction

The binding energy (BE) and the Auger parameter (α') are the two most widely used magnitudes to prove chemical states by XPS. However, the attribution of chemical states may be very ambiguous in systems formed by a minoritary phase dispersed on a support. Thus, for dispersed metals the occurrence of shifts in these parameters at low coverages is well-known.[1−3] For metal oxides, we have recently shown that the BE and α' values of TiO_2 deposited on SiO_2 change by 0.7 and 2.6 eV as the coverage increases.[4] Similar shifts occur for SnO_x ($x = 1$ or 2) supported on SiO_2 and MgO(100).[5] Similarly, in the literature on catalyst systems formed by an active oxide phase deposited on another oxide, there are also references to changes in BE and α' when the active phase is highly dispersed.[6,7] Other materials as oxide solid solutions[8] or mixed oxides of interest as varistors,[9] superconductors,[10] etc. are also systems where changes in the cation and oxygen BEs and Auger KEs are reported as resulting from the integration of a given element in a foreign network with other atoms. However, no clear interpretation of these shifts is usually provided in these studies.

In the present paper we present some new results for TiO_2 deposited on the surface of MgO and Ag and compare them with those of TiO_2/SiO_2. We discuss the observed shifts in BE and α' by simulating the electronic interactions at the interface by means of semiempirical quantum mechanical calculations and cluster models. We calculate the value of the O 2p → Ti 3d gap for the TiO_2 fragment of the clusters and approach the relaxation energy of the photoholes ($\Delta R^{ea} \approx 1/2\Delta\alpha$[11]) by the $(Z + 1)$ approximation. In addition, the effect of the polarization of the surrounding medium on the relaxation energy of the photohole is simulated by a very simple electrostatic model and a proper description of the overlayer−support system. Previous studies in that direction as applied to physisorbed molecules on different supports, especially metals, are those of Nefedov et al.[12,13] We show that the two magnitudes, relaxation energy and band gap, vary in a parallel way. This trend was already shown by Moretti[14] for a large series of semiconductors. The measurement of the Auger parameter is proposed as a method to assess the electronic properties of oxides dispersed on metal or oxide supports.

Experimental Section

TiO_2 has been evaporated from a Ti wire heated in the presence of 2×10^{-6} Torr of oxygen. Under these conditions we have previously shown by XPS that only Ti^{4+} species are formed on Pt(111).[15] This result has been confirmed here for the three substrates on which TiO_2 has been deposited. These substrates were SiO_2−Si(111) (a SiO_2 layer of ∼200 Å of thickness grown on a Si(111) crystal), a MgO(100) single cristal, and a Ag foil. Conditions of preparation and cleaning of the first substrate have been reported previously.[4] The MgO(100) single crystal and the polycrystalline Ag foil, both from Goodfellow, were cleaned in ultrahigh vacuum by succesive ion bombardment and annealing cycles until all impurities initially present on their surfaces were removed as checked by XPS. The Ti/Si, Ti/Mg, and Ti/Ag atomic ratios measured by XPS have been taken as a measurement of the coverage. The samples will be designated as TiO_2/SiO_2-*P*, TiO_2/MgO-*P*, or TiO_2/Ag-*P*, where *P* is the corresponding atomic ratio. XPS spectra after progressive evaporation of TiO_2 have been recorded with a VG-ESCALAB 210 spectrometer working at $\Delta E =$ cte mode at a pass energy of 50 eV. The Mg Kα and Al Kα radiations were used as excitation sources. The binding energy reference was taken at the Mg 1s, Si 2p, and Ag 3d peaks of the substrates taken at 1304.5, 103.4, and 368.3 eV, respectively. To assess the coverage of the substrates, we have also carried out deposition experiments that we have checked simultaneously by XPS and ISS on a Leybold Heraeus LHS10 spectrometer. Here, conditions for XPS analysis were similar. ISS spectra were taken with the same analyzer but with changed polarity

* Corresponding author. Fax: 34-5-4611962. Email: AGUSTIN@CICA.ES.

[⊗] Abstract published in *Advance ACS Abstracts,* August 15, 1996.

S0022-3654(96)00988-4 CCC: $12.00

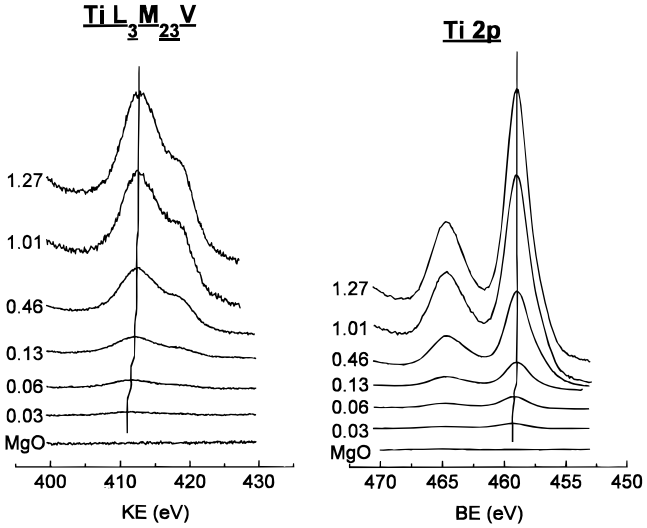

Figure 1. Ti 2p photoelectron (left) and Ti $L_3M_{23}V$ Auger spectra for TiO_2 deposited on MgO(100) at increasing coverages.

in order to detect positive charges. The analyzer was working in the $\Delta E/E$ = cte mode at a retardation ratio value of 3. The He^+ beam had a primary energy of 1000 eV.

UV−vis absorption spectra were recorded for a reference bulk titania in the reflectance mode (R∞) and transformed to a magnitude proportional to the extinction coefficient (*K*) through the Kubelka−Munk function ($F(R\infty)$).[16] The reference sample was a polycrystalline titania in powder form (Degussa P-25). The TiO_2-SiO_2-*P* samples prepared on fused quartz substrates were measured in the transmission mode so that the absorbance (*A*) (which is also proportional to *K*) was recorded directly. Details for this experiment can be found in ref 4. A TiO_2−Ag/SiO_2 sample was prepared by coevaporation of Ag and TiO_2 under 10^{-5} Torr O_2 on the quartz substrate. In this way, it is formed a cermet (ceramic−metal) thin film characterized by an intimate mixture of metallic silver and stoichiometric TiO_2. The TiO_2/Ag molar ratio was 1.55 and the layer thickness 380 Å as estimated according to the method of Gaarestroon et al.[17] In a system of this kind, where the silver forms very small and dispersed particles, there is no specular behavior of the metal and its UV−vis absorption can be examined by transmission in a conventional spectrometer.[18] To evaluate the band gap of the different TiO_2 samples, we have plotted $(Ah\nu)^{1/2}$ or $(F(R\infty h\nu)^{1/2}$ (where $h\nu$ is the photon energy) against $h\nu$. The linear portion of the curve has been extrapolated to an absorption equal to zero.[19]

Valence band photoemission spectra have been taken at the TGM3 line at the BESSY synchrotron in Berlin by using $h\nu$ = 140 eV. Photoemission spectra were recorded at normal emission on an ARIES spectrometer set at constant pass energy with a value of 20 eV. In this case the substrate was the same SiO_2 thin layer (∼200 Å) grown on Si(111). It was cleaned by light bombardment with O_2^+ ions of 400 eV of kinetic energy. Conditions for deposition of TiO_2 were similar to those previously described for this system.[4]

Results

XPS of TiO_2 Deposited on Different Substrates. The three systems have been carefully characterized by XPS, ISS, and EELS (electron energy loss spectroscopy). As a summary of these results, we can conclude that in the three cases TiO_2 is the only form of titanium oxide formed under our experimental conditions. An example of the type of XPS spectra that can be recorded is presented in Figure 1 for TiO_2 deposited on MgO-

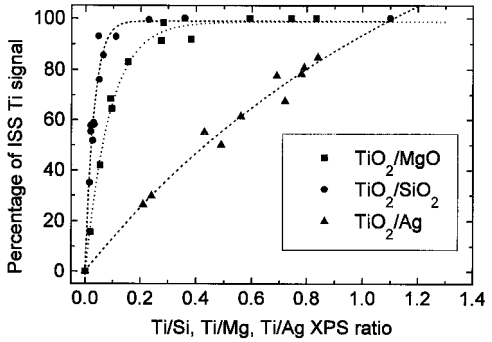

Figure 2. Normalized intensities of the ISS peak of titanium plotted against the Ti/M (M = Si, Mg, Ag) ratios as determined by XPS for TiO_2 supported on SiO_2, MgO, and Ag.

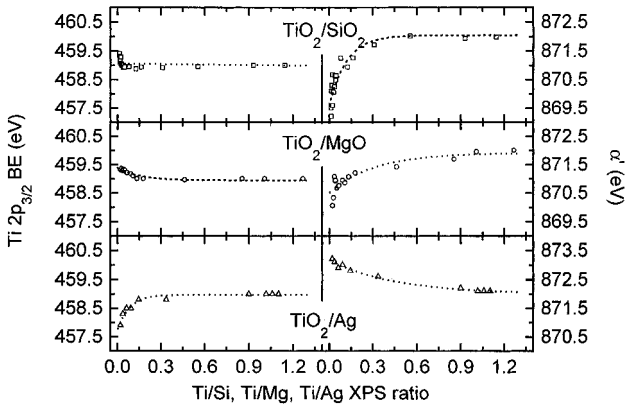

Figure 3. Plots of the Ti 2p BEs and Auger parameters of titanium as a function of Ti/M ratios (M = Si, Mg, Ag) for TiO_2 supported on SiO_2, MgO, and Ag.

(100). Both, the Ti 2p and Ti $L_3M_{23}V$ peaks reported in this figure show a shift in the peak position as the coverage increases. Another feature of these three systems that is relevant for the present study is the spreading ability of TiO_2 on these substrates. Figure 2 shows the plots of the normalized ISS signal of Ti defined as $I_{Ti}/(I_{Ti} + I_{Si,Mg,Ag})$ against the value of *P* measured by XPS. For SiO_2 and Mg this ratio grows very fast, thus showing that TiO_2 spreads on the surface of the substrates.[20] In contrast, on silver the slow increase of the ISS signal of Ti shows that TiO_2 tends to agglomerate on this substrate. However, as will be shown below, at low coverages (i.e., ISS ratio Ti/Ag ≤ 0.3) even in this case there are interface effects that control the photoemission processes of Ti. In this respect, it is worth mentioning that in previous papers,[4,5] we have shown that size effects do not play an important role for the control of photoemission of TiO_2 or SnO supported on graphite.

In Figure 3 we have represented the changes in Ti 2p BE and the Auger parameters (α' = BE of the Ti 2p peak + KE of the Ti $L_3M_{23}V$ Auger peak) for a series of TiO_2-SiO_2-*P*, TiO_2−MgO-*P*, and TiO_2−Ag-*P* samples as a function of *P*.

In the simple approximation introduced by Wagner[11] and Thomas,[21] the shifts in BE and α' can be expressed as $\Delta BE = \Delta\epsilon - \Delta R^{ea}$ and $\Delta\alpha' = 2\Delta R^{ea}$, where $\Delta\epsilon$ is a term related to the eigenvalue of the level undergoing photoemission and the initial state charge distribution, R^{ea} is the extra-atomic relaxation energy of the photohole, and α' is the Auger parameter. By using these equations, we evaluate the ΔR^{ea} and $\Delta\epsilon$ increments with respect to the high coverage situation (high *P* values or bulk TiO_2). The values have been summarized in Table 1. From Figure 3 and Table 1 it is apparent that the influence of the surface substrate modifies the position of the Auger and photoemission peaks of titanium. It is important to bear in mind that according to Figure 2 almost full coverage of the substrate occurs for *P*

TABLE 1: Binding Energy and Modified Auger Parameter Shifts for TiO_2 Supported on Different Substrates and Calculated $\Delta\epsilon$ and ΔR^{ea} Values (in eV)

sample	ΔBE	Δα′	Δϵ	ΔR^{ea}
TiO_2-SiO_2	+0.7	−2.6	−0.6	−1.3
TiO_2-MgO	+0.5	−2.2	−0.6	−1.1
TiO_2-Ag	−1.0	+0.5	−0.75	+0.25

$\simeq$ 0.1 in TiO_2-SiO_2 and TiO_2-MgO. At this value Figure 3 shows that the Ti 2p BE has reached a practically constant value but α has only changed by about 60% of its total variation. On silver this also occur for $P < 0.3$ when the surface of Ag is only partially covered by TiO_2 (cf. Figure 1) and important interface effects are expected.

Also interesting from these experiments is that the variation of the Ti 2p BE and α′ values follows opposite patterns when TiO_2 is deposited on Ag or on SiO_2-MgO. It seems that the metal character of silver and the insulator one of SiO_2 and MgO are factors that influence the photoemission processes of the titanium at the interface. In this respect the fact that the Mg−O bond is rather ionic while the Si−O has a considerable covalent character only contributes to the modification of the magnitude of the change but not its direction at low coverages.

TiO_2 Band Gap Width and Interface Effects. In the previous section we have shown that for small TiO_2 deposits the presence of a metallic or insulator substrate modifies the BE of the Ti 2p peaks and the α′ value of titanium. Therefore, it is also likely that the electronic properties of the layers are also modified as an influence of the substrate. TiO_2 is a wide band semiconductor with a typical band gap of 3.2 eV in its bulk form. This band gap usually increases for a small size of the semiconductor oxide because of quantitation of its electronic levels.[22] In other systems it has been reported that interface effects can contribute to the modification of the electronic properties of a material. Thus, it has been shown that for very thin layers of a semiconductor deposited on a metal, metallization of the former may occur.[23] Also, for small metal particles supported on an insulator, the metal may approach the character of this later.[24]

Here, we want to know if a similar modification of the electronic properties of TiO_2 may be produced when this material is deposited on different substrates. We have investigated this point for the TiO_2/SiO_2 and TiO_2-Ag/SiO_2 systems by UV−vis spectroscopy and by photoemission for TiO_2 supported on SiO_2.

Figure 4 shows the UV−vis spectra of TiO_2/SiO_2-*P* and TiO_2-Ag/SiO_2 cermet samples together with the band gap values, calculated by linear extrapolation of the band edge. The spectrum of bulk TiO_2 is also included for comparison. Although for TiO_2/SiO_2 the observed blue shift (i.e., $E_g = 3.2$ against 3.1 eV measured for the reference TiO_2) of the band gap might be explained in terms of quantum size effects, previous studies on this system have shown that the shift observed in the optical absorption spectra appears higher than expected and that, therefore, the influence of the TiO_2 substrate must be responsible for the observed shift.[4] In this respect we must mention that in our previous paper (ref 4), the gap was obtained by extrapolation of the $(Ah\nu)^2$ curve[25] (A = absorbance) and that the obtained data differ from those obtained here. Moreover, for TiO_2-Ag/SiO_2 the shift (i.e., $E_g = 2.8$ eV) occurs in the opposite direction, thus suggesting that silver exerts an opposite effect than SiO_2 in the modification of the energy gap of TiO_2.

Photoemission experiments confirm that very thin films of TiO_2 deposited on SiO_2 depict a higher band gap than bulk TiO_2. Figure 5 shows the valence band region for different coverages

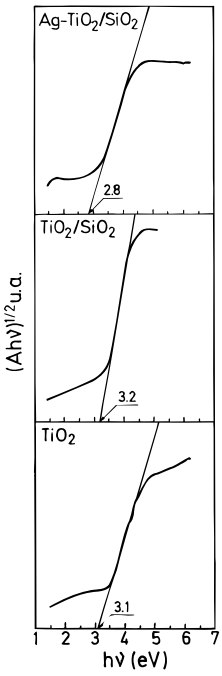

Figure 4. UV−vis absorption spectra of the TiO_2-SiO_2 and TiO_2-Ag/SiO_2 samples showing the position of the band gap edge of TiO_2.

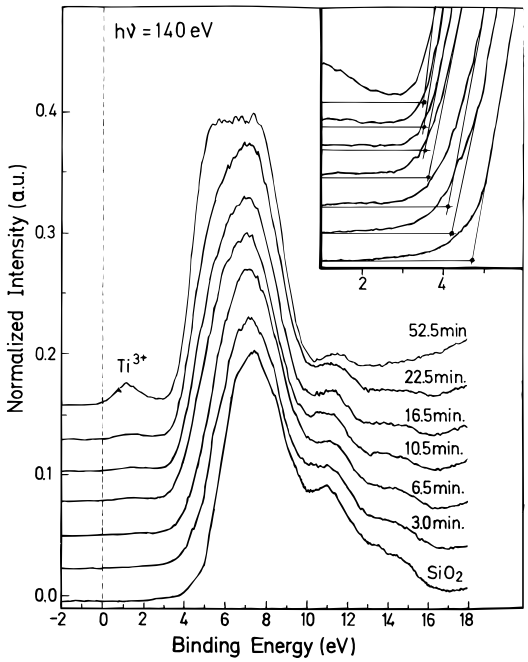

Figure 5. Photoemission spectra ($h\nu = 140$ eV) of the valence band region of TiO_2 deposited on SiO_2 for increasing evaporation times. In the inset note the shift in the position of the band edge as the amount of TiO_2 increases. The peak close to the origin of BE is due to Ti^{3+} species formed at high coverages.

of TiO_2 deposited on SiO_2. The spectra, recorded with $h\nu = 140$ eV, have been aligned with the Si 2p peak at 103.4 eV in order to avoid charging effects in the position of the peaks. At low coverages the spectra are the result of the convolution of the contribution of the valence band spectrum of SiO_2 and that of the TiO_2 deposits. This latter contribution increases with coverage. From this figure, it is apparent that the lines obtained by extrapolation of the band edges cut the BE axis at a position that is closer to the origin of the scale as the TiO_2 coverage increases. Thus, it seems that at low coverages the energy gap of TiO_2 approaches the insulator character of SiO_2. Also, it must be pointed out that at high coverages (i.e., evaporation

SCHEME 1: Cluster Used for INDO/1 Calculations

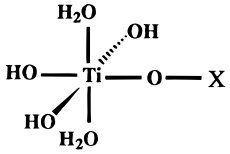

time of 52.5 min) the spectrum clearly shows the formation of a small amount of Ti^{3+} species characterized by a peak at the Fermi level. These species are likely formed because of poor oxidation during deposition, but its presence does not alter the meaning of the comments above on the magnitude of the band gap in the deposited TiO_2.

Quantum Mechanical Modeling and Discussion

In this section, we present a theoretical investigation of the interface effects on the photoemission features of TiO_2 and its electronic properties. Attention is paid to the O 2p → Ti 3d energy gap, E_g, as well as to the extra-atomic relaxation process that takes place as a response of the environment to the Ti 2p core photoionization. We use several cluster models whose electronic structure is calculated by means of semiempirical molecular orbital theory as explained below.

Method and Cluster Models. The simplest cluster contains one Ti−O−X unit as shown is Scheme 1, where X is some entity representative of the support. In those models titanium is surrounded by six or four oxygen atoms in order to account for octahedral or tetrahedral coordination, respectively. Since the dangling bonds at the oxygen atoms would introduce unrealistic features in the electronic levels of the cluster, we have removed these bonds by saturation with hydrogen. The nature of the support is determined by the choice of X. This is $-Si(OH)_3$ for silica, (models I and II) −MgOH for magnesium oxide (model III), and a tetrahedral Ag_4 cluster for silver (model V). By choosing $X = -Ti(OH)_3(H_2O)_2$, we simulate the Ti−O−Ti interaction in bulk titania (model IV). For silica we have considered both tetrahedral (model I) and octahedral (model II) coordinations for Ti, since there is evidence of tetrahedral coordination for titanium in SiO_2 glasses.[26] The distances used are Ti−O = 2.0 Å, Si−O = 1.6 Å, Mg−O = 2.10 Å, Ag−O = 2.0 Å, and Ag−Ag = 2.8 Å.

The molecular orbital calculations for these clusters are based on the semiempirical INDO/1 method.[27] It consists of an all-valence-electron model Hamiltonian whose eigenfunctions and eigenvalues are obtained self-consistently.

Calculation of the Band Gap of Thin TiO_2 Deposits. The band gap is approximated by the energy of the charge transfer from the O 2p to the empty Ti 3d orbitals. For Ti−O−Ti, Ti−O−Mg, and Ti−O−Si this quantity is equivalent to the lowest electronic excitation in the cluster. Thus, it can be estimated as the energy difference of the ground and first excited singlet states of the systems, both calculated self-consistently. The values obtained are 4.89 eV for Ti−O−Si (tetrahedral Ti), 4.84 eV for Ti−O−Si (octahedral Ti), 3.83 eV for Ti−O−Mg, and 3.21 eV for Ti−O−Ti (see first column in Table 2). Apparently, for the TiO_2-SiO_2 and TiO_2−MgO interfaces the energy gap is larger than for titania. This finding agrees with the blue shift of the band gap adsorption edge referred previously for TiO_2 supported on silica and with the shift of the band edge found by photoemission.

For Ti−O−Ag a result of the calculation is that there are filled and unfilled orbitals of silver between O 2p and Ti 3d orbitals and there are several excited states involving excitations of the Ag_4 cluster that are lower in energy than the O 2p → Ti 3d charge transfer. Therefore, in this case we have obtained the lowest optical excitation of the TiO_2 particle from a configuration interaction (CI) calculation that includes all the configurations obtained from single excitations of the 2p orbitals of the central oxygen and filled orbitals of silver to unfilled orbitals of silver and 3d orbitals of Ti. This calculation gives a O → Ti charge-transfer energy of 0.90 eV. This significant decrease of the energy gap obtained by this calculation is consistent with the red shift observed for the TiO_2−Ag structures by UV−vis spectroscopy. The difference between the calculated (0.90 eV) and the experimental (2.8 eV) gaps should be attributed firstly to the simplicity of the cluster model used to describe the TiO_2−Ag interface. To compare the gap calculated for Ti−O−Ag with the band gaps given above for Ti−O−Si and Ti−O−Mg, we have carried out similar CI calculations for the Ti−O−Si, Ti−O−Mg, and Ti−O−Ti models. The results are shown in the second column of Table 2. From these values we conclude that the CI gives values about 2−3 eV larger than the gaps evaluated in the self-consistent calculations. Thus, although the particular value of 0.9 is only indicative, a clear conclusion is that the TiO_2−Ag interface lowers the band gap of TiO_2.

To get a deeper understanding of the effect of the interface and on how the size of the TiO_2 clusters affects the spectroscopic properties, we have obtained the density of states of larger clusters such as those shown in Schemes 2.2−2.4. Owing to the large size of these models, we have used extended Hückel theory (EHT)[28] for the calculations. This method does not lead

TABLE 2: Results of INDO/1 Calculations for Models I−V[a]

model	E_g^{SCF}	E_g^{CI}	R^{ea}	3D	4S	4P	E_{d-s}
I	4.89	7.08	−58.05	0.48	0.02	−0.10	9.19
II	4.84	7.39	−58.54	0.87	0.02	0.08	8.04
III	3.83	6.10	−58.90	0.89	0.02	0.09	8.30
IV	3.21	6.04	−59.15	0.96	0.01	0.01	7.92
V		0.9	−60.56	1.09	0.00	0.01	6.68

[a] E_g^{SCF} is the band gap of the TiO_2 particle calculated as the difference between the ground state and the first singlet excited state, both calculated self-consistently. E_g^{CI} is the band gap obtained as the first O 2p → Ti 3d excitation in a configuration interaction calculation. 3D, 4S, and 4P are changes in 3d, 4s, and 4p orbital populations of the cation when substituting Ti for V^+. E_{d-s} is the energy required to excite one electron from 3d to 4s orbital in V^+, and this quantity is obtained from a CI calculation.

SCHEME 2: Clusters Used for E-H Calculations

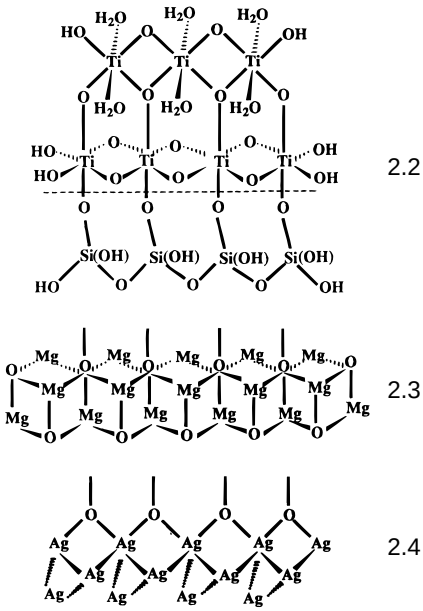

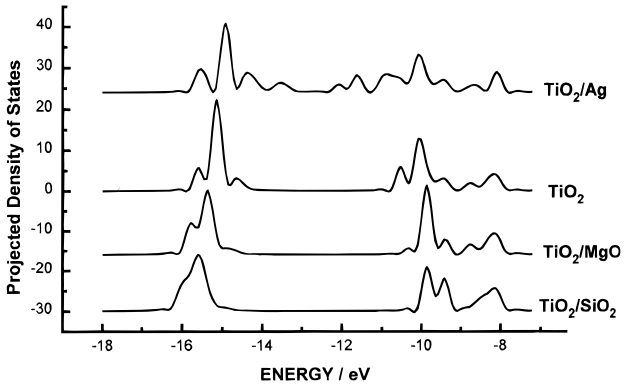

Figure 6. Projected density of states of TiO_2 for the clusters 2.2−2.4 simulating the TiO_2-SiO_2, TiO_2-MgO, and TiO_2-Ag interfaces.

to self-consistent results, and for this reason it is computationally simpler than INDO/1. In Figure 6 we plot the projected density of states of the TiO_2 particles supported on the different surfaces as well as the unsupported particle. For simplicity only valence and conduction bands of the particle are shown. The former, centered about −15.0 eV, is mainly composed of oxygen 2p orbitals. The conduction band, about −10.0 eV, is mainly titanium 3d. The trend is that SiO_2 and MgO enlarge the energy gap between valence and conduction bands. In contrast, silver induces the appearance of some density of states in the gap zone.

These results indicate that the TiO_2 particles become either more insulating or metallic depending on the substrate where they are deposited. As long as we use exactly the same geometry and size for the titania particle in the different models, this electronic effect should be exclusively attributed to TiO_2−support interface interactions.

Calculation of the Extra-Atomic Relaxation Energy. The production of the photohole leaves an unbalanced nuclear charge at the ion site. This increase in positive charge pulls the electron levels of the ion to higher binding energies. Then, it may be energetically favorable for the valence electron charge to be attracted from neighboring atoms into the local potential well in order to screen the core hole. Here, this effect will be described by means of the $Z + 1$ approximation (equivalent core approximation[29]), that is, by assuming that the outer-electron states of the fully relaxed ion Z with a deep core hole are well approximated by the ground state of the $Z + 1$ atom. In our case this approximation implies that the relaxation energy of the environment due to the photoionization of the Ti 2p level can be calculated as the difference between the energies of Ti−O−X and V^+−O−X structures (i.e., the photoionization according to $M[2p^6]3d^0 \rightarrow M[2p^5]3d^0 + e^-$ is equivalent to converting a titanium into a vanadium core). This calculation must account for the different responses of the interface oxygen, depending on the nature of X. The values given in column three of Table 2 show such interface dependence. For the models of Ti−O−Si we obtain −58.05 and −58.54 eV (for the tetrahedral and octahedral coordination, respectively). The relaxation energy for Ti−O−Mg is slightly larger, −58.90 eV. For Ti−O−Ti we obtain −59.15 eV. Finally, the largest relaxation energy, −60.56 eV, is obtained for the TiO_2−silver interface. This dependence of R^{ea} on the support agrees with the shifts in the Auger parameter and Ti 2p binding energies that we measure in our experiments. Moreover, we find that silver, a support that decreases the band gap of the TiO_2 particle, increases the extra-atomic relaxation. In contrast, the interaction with MgO and SiO_2 surfaces, which make the TiO_2 particle more insulating, tends to decrease the relaxation energy of the photohole.

To investigate the screening in our system, we have also looked at the changes in the orbital populations when going from Ti to V^+. The obtained values are given in Table 2 columns 4−7. It is apparent that the 3d population increases almost by one electron in all cases, while the 4s and 4p orbitals do not become more populated in the presence of the core hole. This result agrees with the assumptions of Veal and Paulikas[30] for the relaxation mechanism of transition metal cations. These authors found that the fully relaxed state of the 3d transition metal involves the occupation of an additional d orbital. It is also consistent with fully relaxed self-consistent field calculations of ground state and hole state of molecules[31] or clusters,[32] where population analyses show that the hole state is predominantly compensated by a 3d electron. However, as pointed out by Moretti[33] even through this "local screening" mechanism it can be expected that Ti is sensitive to the nature of the ligands (in our case to the type of TiO_2−X interface). This occurs because of the large degree of hybridization and mixing between the Ti 3d and ligand orbitals. In this respect, it is interesting to address the question of why the photohole is more difficult to relax at low coverages on silica or magnesium oxide than on silver. As shown above for the Ag−TiO_2 interface, the presence of the silver surface induces a Ti 3d density of states below the conduction band as well as a O 2p density of states above the valence band of bulk TiO_2. For this reason, the hybridization energy between V^+ 3d and O 2p levels, which is equivalent to the relaxation energy, is large. Conversely, the interaction with an insulator surface such as SiO_2 and MgO enlarges the gap of the TiO_2 particle, and this leads to a smaller relaxation energy. It is interesting at this point to mention that according to the data in Table 1 and Figures 4−6, there is a correlation between the value of the band gap of the deposited TiO_2 particles and the value of the Auger parameter of Ti. A similar correlation was found by Moretti[14] for a large series of bulk semiconductors. The interest here is that the interaction with the surface of the substrate is the main factor leading to the observed changes in both parameters.

With our model it is also possible to calculate the nonlocal screening states of the system.[30] If we take the fully relaxed core ionized state as the reference, the nonlocal screening can be viewed as an excitation from V^+ 3d + O 2p molecular orbitals to more diffuse V^+ 4s + O 2p combinations. We have done CI calculations to obtain this excitation energy. The values obtained range from 6.68 eV for silver to 9.19 eV for silica and tetrahedral Ti (see values in Table 2). We have found that these nonlocal screening states are sensitive to the environment decreasing in the following order $-Si(OH)_3 > -Mg(OH) > -Ti(OH)_3(H_2O)_2 > Ag_4$. It is likely that those excited states represent the satellite peaks in the XPS spectra, but as long as those features are not well resolved in our spectra at low coverages, we will not discuss them further.

Polarization Energy of the Environment. From our experiments in Figure 3 it is apparent that the change in relaxation energy extends to coverages higher than the corresponding P value around 0.1 (for SiO_2 and MgO $P \approx 0.1$ is equivalent to a monolayer). This means that, besides the direct Ti−O−X interaction, there must be other mechanisms contributing to the screening of the photohole.

The calculations with cluster models presented above show how the interface affects the Ti−O bonds and the response of the first coordination sphere around titanium to create the photohole. We have seen that the contribution of this sphere

to the relaxation of the photohole occurs through the transfer of charge from the oxygens sourrounding the titanium. Besides this process the creation of a photohole induces other effects in the environment. Nefedov et al.[12,13] have studied the influence of the polarization energy and the electrostratic contribution to the extra-atomic relaxation accompanying the photoionization of atoms or molecules physisorbed on surfaces, mainly in relation to experiments of photoemission of adsorbed Xenon. Here, we want to assess the contribution of the polarization energy of the medium as a response of the creation of the photohole. For a continuum this contribution to the polarization energy can be approximated by means of Kirkwood's model.[34] In this model, it is assumed that the dielectric medium is polarized by a charge q placed in a spherical cavity of radius a. The polarization energy is

$$U_h = -\frac{q^2}{2a}\left(1 - \frac{1}{\epsilon}\right) \quad (1)$$

In our case $q = 1$ and the cavity radius (a) is approximated by the Ti−O−Ti, distance of ∼4 Å. This choice enables us to place in the cavity a TiO_6^{8-} cluster. ϵ is the electronic contribution to the dielectric constant, $\epsilon = n^2$, n being the real part of the refraction index. Within this simple model the polarization of the medium in the TiO_2-SiO_2 sample, taken as an example, will have a limit value at low coverage by taking ϵ as 2.25, the electronic dielectric constant of the silica. The difference between the value obtained in this way and that for bulk titania ($\epsilon = 7.56$) gives a change in polarization energy according to eq 1 of 0.56 eV. This simple calculation shows that the change of the contribution of the polarization energy of the environment is not negligible. In fact, by adding this quantity to the difference of relaxation energies between models II and IV, 0.61 eV, one obtains 1.17 eV for the total change of relaxation energy from low to high coverages for the TiO_2-SiO_2 system. This calculation is in rather good agreement with the experimental value of ΔR^{ea}, 1.3 eV.

The other extreme case is for the interface formed between titania and silver. Here, we assume that the dielectric constant for the metal is very large. Then the difference between low coverage ($\epsilon \rightarrow$ infinity) and high coverage results in a small value of $\Delta U_h = 0.23$ eV. This results suggests that bonding effects affecting the first coordination of titanium shell are the most important contribution to account for the difference in relaxation energy in the case of the TiO_2-Ag interface.

Equation 1 is derived for a homogeneous dielectric medium. Therefore, this simple approach seems only appropriate to estimate the changes in relaxation energy for very high or very low coverages where the TiO_6^{8-} units would be inmersed in a TiO_2 or SiO_2 (MgO, Ag) media. Indeed, this model is not useful for intermediate situations where both the support and the layer would contribute to the polarization component of the relaxation energy. To improve the model, we have tried to describe the effect of the interface between the layer, with a dielectric constant ϵ_l, and the support, with a dielectric constant ϵ_s. To do it, we assume that the spherical cavity is embedded in a homogeneous overlayer at a distance "d" of the plane of the interface. In the Appendix we show that, for this model, the changes in the polarization energy according to the thickness of the deposited film (t) can be approximated by the following equation

$$U_i(t) \simeq \frac{\pi q^2}{8t}\left(\frac{1}{\epsilon_l} - \frac{1}{\epsilon_s}\right) \quad (2)$$

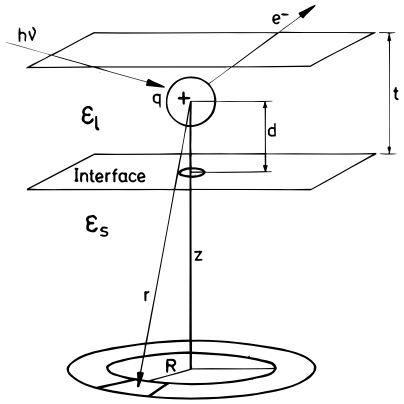

Figure 7. Definition of variables at an interface for the calculation of the polarization contribution to the relaxation energy of photoholes created in an atom of a supported overlayer.

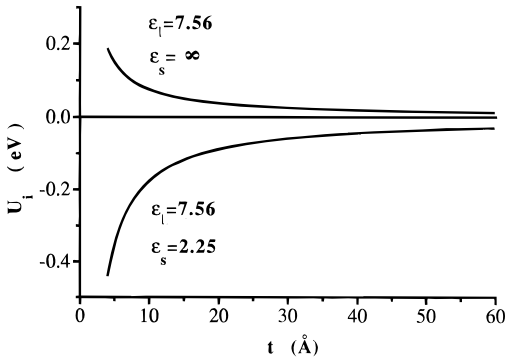

Figure 8. Theoretical plots of the contribution to the relaxation energy of the photoholes due to the polarization of the medium.

It enables the calculation of the changes in the polarization energy as a function of the thickness of the film (t). Figure 8 shows a plot of U against t for the TiO_2-SiO_2 interface where $\epsilon_l > \epsilon_s$. These curves resemble the shape of the curves of the Auger parameter as a function of the thickness of the film (cf. Figure 3). Thus, U_i increases asymptotically from negative values to zero. Conversely, if $\epsilon_s > \epsilon_l$, U_i decreases when t increases. For the TiO_2-SiO_2 interface, the total change in relaxation energy given by eq 2 when going from $t = a$ (a is the cavity radius in Figure 7 taken as the thickness of one monolayer) to $t =$ infinity is 0.44 eV. By adding this quantity to the change in relaxation energy due to the effect of first neighbors, we obtained −1.05 eV, a value that is close to the experimental variation of R^{ea} (−1.3, cf. Table 1). It is also interesting that according to eq 2, 90% of the total polarization energy is reached for a thickness of 40 Å (about 10 layers). For the case of the TiO_2-Ag interface the change in polarization energy when going from $t = a$ to $t \rightarrow$ infinity is only 0.19 eV. This is so because the factor $(1/\epsilon_l - 1/\epsilon_s)$, which appears in eq 2, is small. This means that the difference in polarization energy between bulk titania and titania supported on silver is not important and changes in extra-atomic relaxation energy are mainly accounted for by the effect of the first coordination shell with a very poor contribution of the polarization of the medium. The same conclusion has been reached above by using eq 1 corresponding to a homogeneous medium.

Conclusions

In the previous sections we have shown that the BE of photoelectron peaks and the value of the Auger parameters of Ti^{4+} in thin films of TiO_2 supported on different substrates are strongly influenced by the nature of the support.

In a parallel way we have found that the energy gap can be also altered by the interaction of the thin deposits of TiO_2 with the substrate. When this is an insulator, it tends to increase, and the opposite is found for the case of a metal.

We have simulated the overlayer−substrate interaction by means of molecular orbital calculations and cluster model. This theoretical analysis has shown that for Ti−O−(Mg)Si structures the O 2p−Ti 3d gap increases. The opposite occurs for Ti−O−(Ag_4) structures. Changes in the electron charge distribution at the O and Ti sites may also account for the initial state changes of the photoemission process. The relaxation energy of the photohole has been calculated by the $(Z + 1)$ approximation. This stems from the different energies of the structures Ti−O−X and V^+−O−X. The values obtained follow the same tendency as the experimental $\Delta\alpha'$ calculated as a difference between the low and high coverage situations. Simultaneously, an analysis of the electron density distribution before and after the photoemission process shows that the relaxation of the photohole proceeds through a "nonlocal" screening mechanism.[30] The previous contribution to the relaxation process is related to the bond formation between support and overlayer through oxygen atoms. Another contribution, which is not restricted to the first monolayer, comes from the polarization of the medium. This is approximated through an electrostatic approach, and the obtained results are similar to the experimental values.

All these results show the high sensitivity of the BE and Auger parameter values for oxides of ions of the beginning of the transition series to the interaction with another material. Shifts in these parameters may amount up to several electronvolts even if the formal oxidation state of the cation is the same. This may be important for the characterization of materials consisting of a phase dispersed on a substrate, as often happens in catalysts, sensors, etc.

Acknowledgment. We thank the DGICYT (Project PB93-0183) and CICYT (Project MAT94-1039-C02-01) for financial support. The photoemission experiments have been carried out at BESSY thanks to a grant from the HCM program of the EC.

Appendix

Interface Contribution to the Polarization of a Dielectric by a Point Charge. Let us consider a point charge q, which polarizes a medium with a dielectric constant ϵ. By simple electrostatic considerations, we know that the polarization energy is

$$U = -\frac{1}{8\pi}\int_v \left(1 - \frac{1}{\epsilon}\right) F^2 \, dv \qquad (A.1)$$

where $F = q/r^2$ and the integration extends to an infinite volume occupied by the dielectric.

To calculate the polarization energy of a medium that contains a plane interface between two materials with dielectric constants ϵ_l and ϵ_s, we assume that the point charge is inside a spherical cavity at a distance d from the interface as depicted in Figure 7. We will assume that d is equivalent to t, the thickness of the deposited film. This approximation is reasonable, since most electrons detected by XPS proceed from the first layers of the materials, the contribution from inner layers being attenuated according to the probability of inelastic scattering of photoelectrons. When $t \rightarrow \infty$, we have a homogeneous dielectric and the polarization energy is given by eq 1. To evaluate U under the presence of the interface, we calculate the interaction between q and the dielectric medium, which is on the other side of the plane, U_s (i.e., the support). Using cylindrical coordinates, it results in the following simple equation

$$U_s = -\frac{q^2}{8}\left(1 - \frac{1}{\epsilon_s}\right)\int\int \frac{1}{(R^2 + z^2)^2} 2\pi R \, dR \, dz \qquad (A.2)$$

where $R \in (0, \infty)$, $Z \in (d, \infty)$ and the meaning of the different variables is evident from the scheme.

By doing this integration, one finds that

$$U_s = -\frac{\pi q^2}{8d}\left(1 - \frac{1}{\epsilon_s}\right) \qquad (A.3)$$

The polarization energy of the deposited material U_f can be calculated by assuming a very large thickness of the film (i.e., infinity) and by subtracting from the energy of the homogeneous environment with dielectric constant ϵ_l (given in eq 1) a term analogous to A.3 where ϵ_l replaces ϵ_s.

$$U_f = -\frac{q^2}{2a}\left(1 - \frac{1}{\epsilon_l}\right) + \frac{\pi q^2}{8d}\left(1 - \frac{1}{\epsilon_l}\right) \qquad (A.4)$$

Formally, the total polarization energy, $U = U_f + U_s$ can be written as the energy of a homogeneous dielectric, U_h (eq 1 for a dielectric constant ϵ_l), plus a polarization energy due to the interface, U_i, where U_i is given by

$$U_i = \frac{\pi q^2}{8d}\left(\frac{1}{\epsilon_l} - \frac{1}{\epsilon_s}\right) \qquad (A.5)$$

and

$$U = U_f + U_s = U_h + U_i$$

If one takes into account the discrete thickness of the film, changes in polarization energy according to the thickness of the deposited film (t) would be equivalent to $U - U_x$, where

$$U_x = -\frac{\pi q^2}{8a}\left(1 - \frac{1}{\epsilon_l}\right) \qquad (A.6)$$

represents the polarization of the space beyond the cavity where there is actually no deposited material (i.e., vacuum).

Then the polarization energy of the film would be given by

$$U_T = U_h - U_x + U_i$$

where U_h and U_x do not change as a function of d (here, we will assume that it is equivalent to the thickness of the deposited layer t) and changes in polarization energy would depend exclusively on U_i given by eq A.5. By replacing d by t in this formula and after approximation,

$$U_i(t) \simeq \frac{\pi q^2}{8t}\left(\frac{1}{\epsilon_l} - \frac{1}{\epsilon_s}\right)$$

as in eq 2.

References and Notes

(1) Mason, M. B. *Phys. Rev. B* **1983**, *27*, 748.
(2) Vijayakrishnanm, V.; Rao, C. N. *Surf. Sci.* **1991**, 255.
(3) Espinós, J. P.; Fernández, A.; González-Elipe, A. R.; Munuera, G. *Surf. Sci.* **1991**, *251/252*, 1012.
(4) Lassaletta, G.; Fernández, A.; Espinós, J. P.; González-Elipe, A. R. *J. Phys. Chem.* **1995**, *99*, 1484.
(5) Jiménez, V.; Fernández, A.; Espinós, J. P.; González-Elipe, A. R. *Surf. Sci.* **1996**, *350*, 123.
(6) Fernández, A.; Caballero, A.; González-Elipe, A. R. *Surf. Interface Anal.* **1992**, *18*, 392.
(7) Xie, Y. C.; Tang, Y. Q. *Adv. Catal.* **1990**, *37*, 1.

(8) Moretti, G.; Cimino, A.; Minelli, G.; de Angelis, B. A. *J. Electron Spectrosc. Relat. Phenom.* **1986**, *40*, 85.
(9) Tanaka, Sr.; Akita, Ch.; Ohashi, N.; Kawai, J.; Haneda, H.; Tanaka, J. *J. Solid State Chem.* **1993**, *105*, 36.
(10) Brundle, C. R.; Fowler, D. E. *Surf. Sci. Rep.* **1993**, *19*, 143.
(11) Wagner, C. D. *Faraday Discuss. Chem. Soc.* **1975**, *60*, 291.
(12) Nefedov, V. I. *J. Electron Spectrosc. Relat. Phenom.* **1993**, *63*, 355.
(13) Nefedov, V. I.; Fedorova, I. S. *J. Electron Spectrosc. Relat. Phenom.* **1995**, *71*, 233.
(14) Moretti, G. *J. Electron Spectrosc. Relat. Phenom.* **1990**, *50*, 289.
(15) Asensio, M. C.; Kerkar, M.; Woodruff, D. P.; de Carvalho, A. V.; Fernández, A.; González-Elipe, A. R.; Fernández-García, M.; Conesa, J. C. *Surf. Sci.* **1992**, *273*, 31.
(16) Klier, K. *Catal. Rev.* **1967**, *1*, 207.
(17) Waldo, R. A.; Militella, M. C.; Gaarestroon, S. W. *Surf. Interface Anal.* **1993**, *20*, 3.
(18) Taga Y. *Surf. Interface Anal.* **1994**, *22*, 149−155.
(19) Salvador, P. *Sol. Energ. Mater.* **1982**, *6*, 241.
(20) Bardi, U. *Appl. Surf. Sci.* **1991**, *51*, 89.
(21) Thomas, T. D. *J. Electron Spectrosc. Relat. Phenom.* **1980**, *20*, 117.
(22) (a) Kormann, C.; Bahnemann, O. W.; Hoffmann, R. M. *J. Phys. Chem.* **1988**, *92*, 5196. (b) Kavan, L.; Stoto, T.; Grätzel, M.; Fitzmaurice, D.; Shklover, V. *J. Phys. Chem.* **1993**, *97*, 9493. (c) Ampo, M.; Shima, T.; Kodama, S.; Kubokawa, Y. *J. Phys. Chem.* **1987**, *91*, 4305.
(23) Zhang, S. B.; Cohen, M. L.; Lonie, S. G. *Phys. Rev. B* **1986**, *34*, 768.
(24) Aiyer, H. N.; Vijayakrishnann, V.; Subbanna, G. N.; Rao, C. N. R. *Surf. Sci.* **1994**, *313*, 392.
(25) Zhang, D. H.; Brodie, D. E. *Thin Solid Films* **1992**, *213*, 109.
(26) Stakheev, A. Y.; Shpiro, E. S.; Apijok, J. *J. Phys. Chem.* **1993**, *97*, 5668.
(27) Ridley, J.; Zerner, M. *Theor. Chim. Acta* **1973**, *32*, 111.
(28) Hoffmann, R. *J. Chem. Phys.* **1963**, *39*, 1397.
(29) (a) Jolly, W. L.; Hendrickson, D. *J. Am. Chem. Soc.* **1970**, *92*, 1863. (b) Jolly, W. L. *J. Am. Chem. Soc.* **1970**, *92*, 3260.
(30) Veal, B. W.; Paulikas, A. P. *Phys. Rev. B* **1985**, *31*, 5399.
(31) Ruscic, B.; Goordna, G.; Berkowitz, J. *J. Chem. Phys.* **1983**, *78*, 5443.
(32) Gunnarsson, O.; Schonhammer, K. *Phys. Rev. B* **1980**, *22*, 3710.
(33) Moretti, G. *Surf. Interface Anal.* **1990**, *16*, 159; **1991**, *17*, 352.
(34) Kirkwood, J. G. *J. Chem. Phys.* **1934**, *2*, 351.

JP960988C